Supplementary material

Structure and conformation study of the O-antigen from the lipopolysaccharide of *Cupriavidus metallidurans* CH34

Anna Notaro[1], Adele Vanacore[2], Antonio Molinaro[2], Immacolata Speciale[1], and Cristina De Castro[1],*

1   Department of Agricultural Sciences; Via Università 100, 80055 Portici, Italia)
2   Department of Chemical Sciences, Via Cintia 4, 80126 Napoli (Italy)
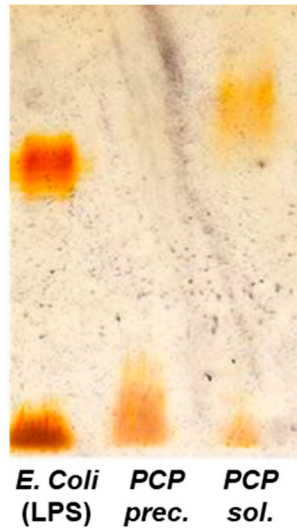*   Correspondence: decastro@unina.it.

Figure S1. SDS-PAGE (15%) of the fraction of the PCP extractions, stained with Silver staining. In comparison with pure LPS of E. coli (positive control of the carbohydrate staining), the (R)-type LPS was found in the PCP precipitate (PCP prec.), while the (S)-type LPS was found in the phenol phase (PCP sol.)
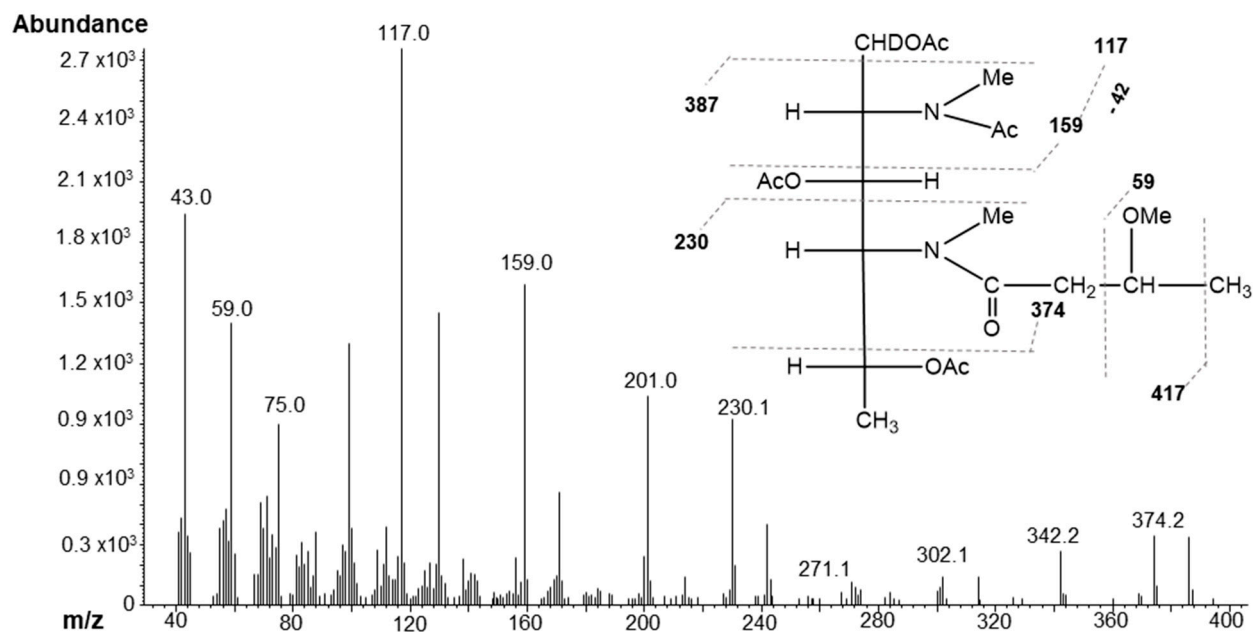
Figure S2. EI-MS spectrum of the Qui2NAc4NHBA (retention time: 36 min), a sugar component of the O-antigen of *Cupriavidus metallidurans* CH34. Fragment at 230 *m/z* and 374 *m/z* are consistent with a Qui2NAc4N bearing a 3-hydroxy-butyric acid at C-4 amino group.
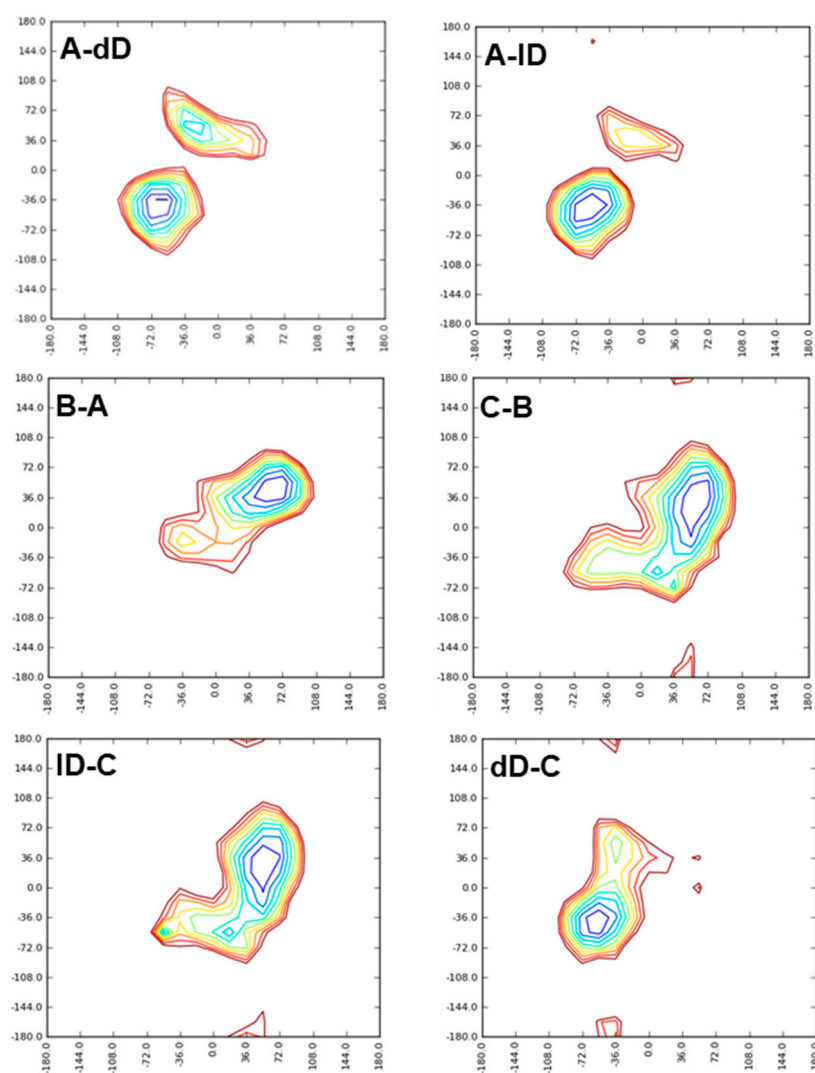
Figure S3. [1]H and ^{13}C heteronuclear spectra of O-antigen of *Cupriavidus metallidurans* CH34 (600 MHZ, 318 K, in D₂O). Overlay of HSQC (black/dark grey) and HMBC (light grey) spectra detailing: **a)** the anomeric and the ring proton regions; **b)** the region containing the methylene signals of the 3-hydroxybutyric acid (HBA) and the long range correlation connecting the methyl group of the HBA to its methylene signals; **c)** the density of the CH₃ of the HBA at 23.7 ppm. Letters used for the annotation of the cross peaks follow the system of Table 1. In red are highlighted the HMBC correlations that were fundamental to define the O-antigen structure.

Figure S4. Φ (abscissa) and Ψ (ordinate) flexible maps calculated for the glycosidic linkages present in the O-antigen of *Cupriavidus metallidurans* CH34. Contours are drawn at increments of 0.2 kJ/mol above the absolute minimum found. Monosaccharides are labelled with the letters used during NMR attribution (Table 1). Lowercase letters indicate the absolute configuration of the residue (d means D-configured, l means L). Global minima values are reported in Table S1. Φ and Ψ are defined according to the NMR formalism, $\Phi = H_1\text{-}C_1\text{-}O\text{-}C'n$; $\Psi = C_1\text{-}O\text{-}C'n\text{-}H'n$.
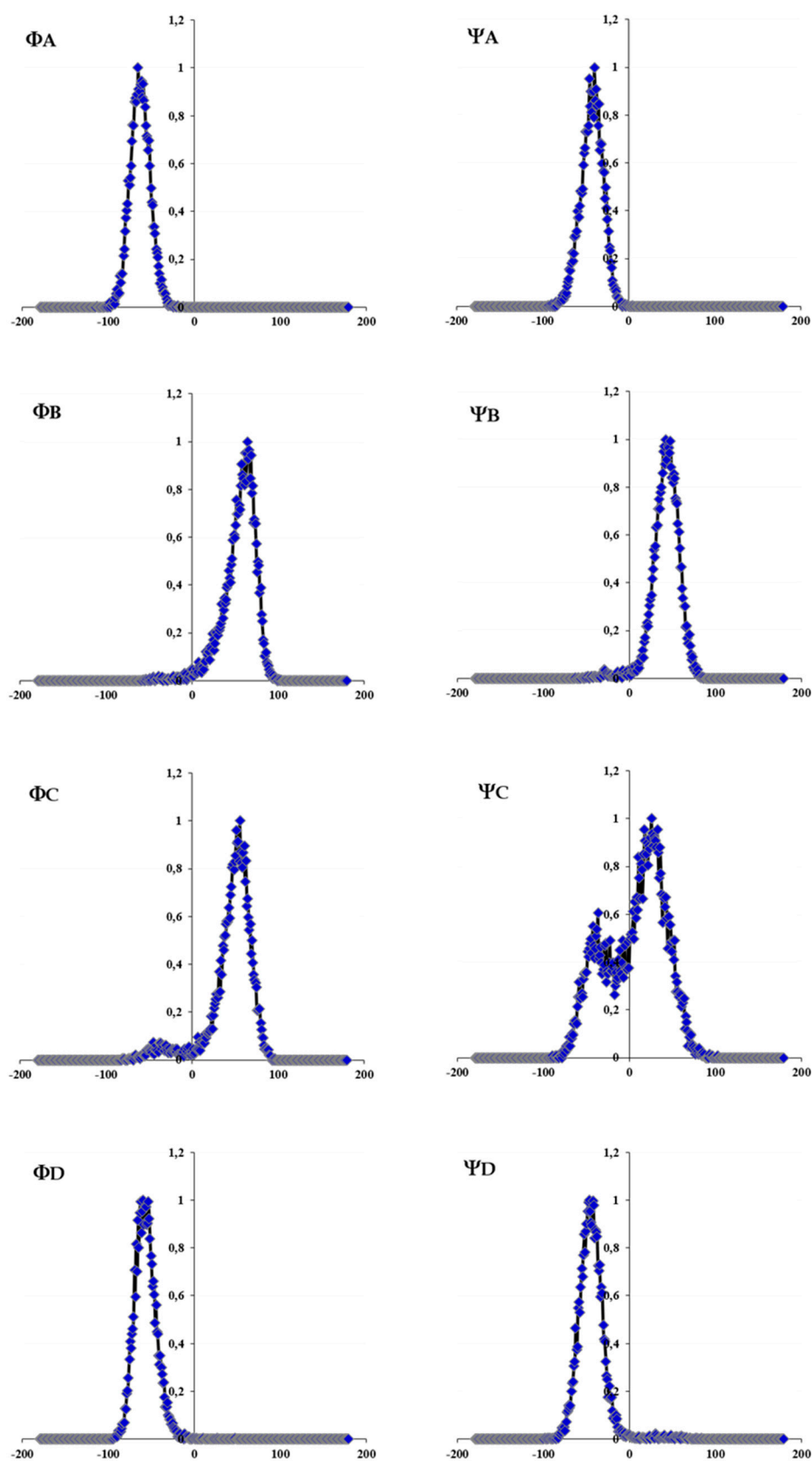
Figure S5. Frequency count graphs of Φ and Ψ values of the glycosidic junction of the ᴅ-**penta**: B-A-C-dD-B. Graphs were made by OriginPro 8.5 program. Φ and Ψ are defined according to the NMR formalism, $\Phi = H_1\text{-}C_1\text{-}O\text{-}C'n$; $\Psi = C_1\text{-}O\text{-}C'n\text{-}H'n$

Table S1. Values found for the glycosidic linkages of six disaccharides by using a molecular mechanic approach. Angles are defined as follows: $\Phi = H_1\text{-}C_1\text{-}O\text{-}C'_n$; $\Psi = C_1\text{-}O\text{-}C'_n\text{--}H'_n$.

	Φ	Ψ
A-dD	-64	-43
A-lD	-58	-39
B-A	63	46
C-B	58	29
lD-C	54	29
dD-C	-56	-41

Table S2. Dihedral angle values in the XR-ray format ($\Phi = O_5\text{-}C_1\text{-}O\text{-}C'_n$; $\Psi = C_1\text{-}O\text{-}C'_n\text{-}C'_{n+1}$) or in the NMR format ($\Phi = H_1\text{-}C_1\text{-}O\text{-}C'_n$; $\Psi = C_1\text{-}O\text{-}C'_n\text{-}H'_n$) of the different glycosidic junctions of the two conformers, named D-penta-A and D-penta-B. These values were deduced from the frequency counts graphics (Figure S5) and they were feed into POLYS program to evaluate which helix conformation (defined from the parameter n) could assume the glycan. Typically, the first calculated n value is never an integer number, and by successive optimization of the dihedral angle values, it is fitted into an integer value that indicates the number of repeating units necessary to define a helix turn.

		D-penta-A			
n	dihedral	B-A	A-D	D-C	C-B
3,71$_{XR}$	Φ	-51,6	52,9	56,3	-70,1
	Ψ	164,3	80,9	-168,8	-96,7
4$_{XR}$	Φ	-50,38	54,86	56,57	-70,52
	Ψ	166,40	82,78	-167,18	-94,84
4$_{NMR}$	Φ	66,8	-62,6	-65,0	46,6
	Ψ	45,8	-39,0	-47,0	25,4
		D-penta-B			
2,41$_{XR}$	Φ	-51,6	52,9	56,3	-70,1
	Ψ	164,3	80,9	-168,8	-164,7
2$_{XR}$	Φ	-57,12	46,40	57,26	-72,25
	Ψ	157,57	74,60	-174,24	-170,97
3$_{XR}$	Φ	-46,19	59,26	55,36	-67,99
	Ψ	170,89	87,07	-163,48	-158,55
2$_{NMR}$	Φ	60,01	-71,0	-64,28	44,89
	Ψ	36,94	-47,15	-54,02	-50,75
3$_{NMR}$	Φ	70,94	-58,14	-66,18	49,15
	Ψ	50,25	-34,69	-43,26	-38,32